TU Delft

Delft University of Technology

Document Version
Final published version

Licence
CC BY

Citation (APA)
Kolganov, A. A., Bougueroua, S., Gaigeot, M. P., Conley, M. P., & Pidko, E. A. (2026). Graph theory-based exploration of structure and dynamics of surface organometallic catalysis. *Journal of Catalysis*, *453*, Article 116521. https://doi.org/10.1016/j.jcat.2025.116521

Important note
To cite this publication, please use the final published version (if applicable).
Please check the document version above.

Copyright
In case the licence states “Dutch Copyright Act (Article 25fa)”, this publication was made available Green Open Access via the TU Delft Institutional Repository pursuant to Dutch Copyright Act (Article 25fa, the Taverne amendment). This provision does not affect copyright ownership.
Unless copyright is transferred by contract or statute, it remains with the copyright holder.

Sharing and reuse
Other than for strictly personal use, it is not permitted to download, forward or distribute the text or part of it, without the consent of the author(s) and/or copyright holder(s), unless the work is under an open content license such as Creative Commons.

Takedown policy
Please contact us and provide details if you believe this document breaches copyrights.
We will remove access to the work immediately and investigate your claim.

This work is downloaded from Delft University of Technology.

Journal of Catalysis 453 (2026) 116521

Contents lists available at ScienceDirect

Journal of Catalysis

journal homepage: www.elsevier.com/locate/jcat

Research article

Graph theory-based exploration of structure and dynamics of surface organometallic catalysis☆

Alexander A. Kolganov [a], Sana Bougueroua [b], Marie-Pierre Gaigeot [b,c], Matthew P. Conley [d], Evgeny A. Pidko [a,*]

[a] Inorganic Systems Engineering group, Department of Chemical Engineering, Faculty of Applied Sciences, Delft University of Technology, Delft, the Netherlands
[b] Université Paris-Saclay, Univ Evry, CY Cergy Paris Université, CNRS, LAMBE, UMR8587, 91025 Evry-Courcouronnes, France
[c] Institut Universitaire de France (IUF), 75005 Paris, France
[d] Department of Chemistry, University of California, Riverside, USA

ARTICLE INFO

Keywords:
Surface organometallic chemistry
Configurational exploration
Graph theory
Molecular dynamics simulations

ABSTRACT

Capturing the dynamic behavior of active sites on complex, amorphous supports is a significant challenge in modeling single-site catalysts, particularly in surface organometallic catalysts. These systems are characterized by a well-defined chemical bonding pattern that coexists with the fluxionality of ancillary ligands and the inherent complexity of the support. Here, we present a conceptual workflow that integrates reactive molecular dynamics with advanced graph theory-based analysis to systematically explore the configurational space of supported catalysts. First, we used enhanced molecular dynamics to overcome local energy barriers and generate a diverse ensemble of structures. Then, we applied graph-based algorithms to distinguish truly distinct isomers from mere conformers and rotamers. Applying this approach to the model system of 1,1′-bis(n-butyl-cyclopentadienyl) zirconium dihydride on a dehydrated amorphous silica model, our method reveals the significant role of local silica strain in shaping the ensemble of active site configurations: catalysts grafted on silanol groups with strained confinement exhibit a diverse array of reaction pathways and significant energy stabilization, whereas less-strained environments yield a more restricted set of accessible configurations. This work demonstrates that combining molecular dynamics with graph theory provides an intuitive framework for unraveling the complex, fluxional behavior of supported catalysts.

1. Introduction

The development of advanced predictive models in catalysis requires a comprehensive understanding of the molecular structure of active sites, their reactivity, and their evolution under operating conditions. [1,2] Traditionally, it has been assumed that a catalyst's behavior under non-equilibrium conditions can be adequately described by the intrinsic properties of a dominant equilibrium configuration of a single active site. Despite being practical, such a reductionist approach fails to capture the complex and diverse behaviors observed in real-world catalytic systems. [3–7] To establish a more complete mechanistic description of catalytic processes, a shift towards the dynamic representation of the catalytic ensembles is necessary. In other words, the catalyst models should account for the fluctuations in structure and stoichiometry within the catalytic ensembles under the operating conditions, giving rise to the coexistence of multiple states, which together determine the activity, stability and selectivity of the catalyst. [8].

Structural dynamics, commonly referred to as fluxionality, is a well-established phenomenon in supported metal clusters, [8,9] where non-directional bonds enable significant configurational freedom under catalytic conditions. Molecular organometallic complexes can also exhibit fluxional behavior through such mechanisms as ligand hemilability or conformational dynamics. [10–17] Similarly, variations in the coordination environment of surface sites contribute to the fluxionality observed in supported catalysts. For example, amorphous silica, which is frequently used as a support in surface organometallic catalysts (SOMC) and single-atom catalysis, provides a range of coordination microenvironments that stabilize active sites. [18,19] Consequently, catalytic performance may be influenced by an array of species with diverse reactivity rather than by a single, uniform active site [18,20].

☆ This article is part of a special issue entitled: 'Molecular Dynamics in Catalysis' published in Journal of Catalysis.

* Corresponding author.
E-mail address: E.A.Pidko@tudelft.nl (E.A. Pidko).

https://doi.org/10.1016/j.jcat.2025.116521
Received 12 August 2025; Received in revised form 19 October 2025; Accepted 24 October 2025
Available online 30 October 2025
0021-9517/© 2025 The Author(s). Published by Elsevier Inc. This is an open access article under the CC BY license (http://creativecommons.org/licenses/by/4.0/).

Understanding fluxional active sites requires extensive exploration of both the chemical and configurational spaces to locate the minima on the potential energy surface (PES). Characterizing and exploring the PES is a complex and tedious task. Traditionally, computational studies in catalysis have addressed this challenge by manually investigating various active site configurations, relying heavily on expert knowledge and chemical intuition. [21,22] This approach often limits the analysis to the reactivity domains anticipated by experts. However, recent advancements in computational chemistry offer automated methodologies to reduce this inherent bias, thereby broadening the scope of mechanistic analyses. [8,23,24].

Various global optimization techniques have been developed to identify the global minima of complex structures and to explore dynamic ensembles. [25–34] These methods are particularly effective for predicting ensembles in supported metallic clusters, where chemical bonding is either non-directional or highly delocalized. The resulting structural flexibility essentially permits the "juggling" of atoms to uncover different active site configurations. However, applying these techniques to more chemically complex systems, such as molecular (surface) organometallic catalysts supported on amorphous materials, presents additional challenges due to the directional nature of covalent bonds in ancillary ligands. Conventional approaches may inadvertently break covalent bonds, yielding structures that are not chemically accessible from the initial guess. In such cases, the exploration may need to follow the PES in a more chemically relevant manner, either through the artificial force-induced reaction method [35–37] or *via* reactive molecular dynamics. [38–42].

Extracting detailed information about the unique structures sampled in reactive molecular dynamics trajectories is a challenging task. Tracking the evolution of the three-dimensional structure of catalysts over time and identifying distinct features and connectivity changes is often difficult when relying solely on conventional analyses of coordinates within trajectories. Algorithmic graph theory offers a robust alternative by using topological graphs to monitor structural changes and generate comprehensive global statistics. [43] In this framework, a graph encodes the molecular-level properties of matter through vertices and edges that represent specific chemical interactions. Typically, vertices correspond to individual atoms, while edges represent chemical bonds, including both inter- and intramolecular interactions.

Molecular graphs defined in two dimensions (2D-MolGraphs) provide powerful tools to differentiate between unique isomers, effectively filtering out all conformers and rotamers in trajectories of 3D structures. The use of 2D-MolGraphs to model intra- and intermolecular interactions is now well-established. [43–48] A key element in the mathematical analysis of molecular graphs is the concept of isomorphism, which enables the identification of constitutional isomeric forms within a given molecular system. [49].

Herein we present an approach for the structural exploration of supported catalytic ensembles by combining *ab initio* molecular dynamics (MD) methods with advanced graph theory-based post-processing tools for comprehensive trajectory analysis. To illustrate this approach, a silica-supported 1,1′-bis(n-butyl-cyclopentadienyl)zirconium dihydride single-site catalyst was selected as a representative model system for this study. Catalysts of this type are traditionally employed in olefin polymerization [50] and show promise in chemical plastic upcycling applications. [51–53].

2. Computational details

Models. All simulations were carried out using a fully periodic amorphous silica surface 2.1 nm × 2.1 nm model with a surface coverage of 1.1 silanol per nm^2 proposed by Comas-Vives. [54] This surface represents amorphous silica dehydrated at 973 K under vacuum. The unit cell formula of this model can be described as $Si_{70}O_{194}(SiOH_{bottom})_{31}(SiOH_{surface})_5$. A 30 Å vacuum layer above the silica surface was added to prevent spurious interactions between neighboring periodic images.

Electronic structure calculations were performed in the CP2K 2022.1 software [55] using the Gaussian-Plane Waves method. [56] The PBE(D3BJ) functional [57,58] was used to describe the exchange–correlation energy term. Plane wave energy cutoff of 450 Ry was set for the plane wave part of basis set. DZVP-MOLOPT-SR-GTH basis set was employed to describe valence electrons of Si, O, and H atoms, while the TZVP-MOLOPT-SR-GTH basis set was used to describe the valence electrons of Zr. [59] This method was applied for both MD runs and geometry optimizations. The latter were carried out using Broyden–-Fletcher–Goldfarb–Shanno (BFGS) algorithm naturally seeks points where the gradient is close to zero and all eigenvalues of the Hessian are positive, which defines a local minimum.

To explore the configurational space of the systems under consideration, ab initio molecular dynamics (aiMD) simulations were conducted in the NVT ensemble using the Nosé-Hoover chain thermostat with a time constant of 15 fs. Each aiMD trajectory was integrated over 5 ps with a time step of 0.5 fs. Initial velocities were randomly generated from and scaled to match the target temperature. The mass of hydrogen atoms was set to 2.014 u (deuterium mass) to enable a larger integration time step. One aiMD simulation was conducted at 353 K, and three additional simulations were performed at 773 K to accelerate the escape from the initial local minimum. Furthermore, we employed molecular dynamics with velocity softening for the first 100 MD steps, as implemented in CP2K. This method initializes velocities along low-curvature directions, enabling the MD trajectories to quickly overcome small energy barriers and access neighboring basins. [60] For each MD simulation, a different initial seed for the global pseudorandom number generator was assigned to ensure unique initial velocities in each run. In total, 10 MD simulations were performed for each structure: one at 353 K, three at 773 K, and six additional velocity softening runs. All frames from these simulations (100,000 total frames) were used for the subsequent graph-theory analysis without discarding any equilibration period.

Molecular dynamics trajectories analysis was carried out with the graph-theory-based software GaTewAY, which transforms 3D Cartesian coordinates into 2D-MolGraphs. In this section, we will briefly outline the functionality of GaTewAY. For a more detailed overview see refs. [43,45,47].

The core idea behind GaTewAY is to convert a molecule from a 3D Cartesian coordinate set into a 2D graph without retaining any spatial orientation information, to effectively distinguish isomers from conformers and rotamers. In this workflow, each MD frame is converted into a graph, [45] $\boldsymbol{G} = \boldsymbol{(V, E_C, E_O)}$ where:

$\boldsymbol{V}$: is the set of all atoms present in the frame, where each atom corresponds to a node in the graph $\boldsymbol{G}$.

$\boldsymbol{E_C}$: is the set of covalent bonds, where each bond is represented as an undirected edge. A covalent bond is formed between a pair of atoms [*a*, *b*] with respective Cartesian coordinates (x_a, y_a, z_a) and (x_b, y_b, z_b), if the Euclidean distance

$$D = \sqrt{(x_a - x_b)^2 + (y_a - y_b)^2 + (z_a - z_b)^2}$$

is less than cutoff distance D_r. For covalent bonds, the algorithm defines the D_r distance by the sum of covalent radii of atoms a and b with an additional margin of 15 % of this sum.

$\boldsymbol{E_O}$: is the set of coordination interactions (defined as "organometallic interaction" in GaTewAY) between Zr and other elements (C, O, H) where each interaction is represented as an undirected edge in the graph *G*. Note that for some pairs of atoms, either covalent or coordination bond can be defined, depending on the interatomic distance.

The analysis excluded any hydrogen bonding. The lower part of the surface is saturated with silanol groups, forming an extensive and rapidly changing network of hydrogen bonds during the MD runs, and the variations in these hydrogen bonds are irrelevant for the purposes of the current analysis.

The Cartesian atomic positions obtained from the MD trajectory are used to construct these mixed graphs at each time step of the dynamics. Once these graphs are generated, changes along the MD trajectories are analyzed by performing isomorphism checks to compare the graphs from one snapshot to another. The combined results from the ensemble exploration are then compiled into a network (graph of transitions), where the nodes represent unique isomers, and the edges denote transitions observed between structures in the MD trajectories. The unique structures detected within MD trajectories by GaTewAY are not necessarily minima on the potential energy surface (PES); they may instead be located on the slopes leading to the same stationary points. Consequently, all detected unique structures within the trajectory were optimized, and the resulting ensemble network was simplified. The simplification algorithm as well as constants and assumptions that were used in this work for graph-theory analysis are described in the section S1of the SI.

3. Results and discussion

In this study, we apply our methodology to a system featuring 1,1′-bis (n-butyl-cyclopentadienyl)zirconium dihydride ($^{Bu}Cp_2ZrH_2$) supported on amorphous silica. Previously Culver et al. demonstrated the formation of $^{Bu}Cp_2ZrH^+\ldots[HAl{\equiv}]^-$ sites on a passivated alumina surface uniquely active in ethylene polymerization. [50] In the current model, the formation of a similar active site can be envisaged via the recombination of the $[^{Bu}Cp_2ZrH_2]_2$ dimer hydride with a proton from a silanol group (Fig. 1a).

Two distinct silanol sites served as anchoring points for the organometallic pre-catalyst: a silanol group (denoted as SiOH-1) bonded to a silicon atom in a distorted tetrahedral geometry and surrounded by strained SiO_4 moieties, and a silanol group (SiOH-2) with a nearly perfect tetrahedral geometry (Fig. 1b). The starting point for the aiMD configurational exploration was the resulting surface complex $^{Bu}Cp_2ZrH@SiO_2$ as depicted in Fig. 1c.

The overall workflow for the structural search of the active site ensemble is schematically illustrated in Fig. 2. This approach is inspired by our previous work, in which k-medoid clustering based on Cartesian coordinates was used to search configurations in ab initio velocity-softening MD trajectories for Cu_3O_3/MOR. [61] However, in the present study, such clustering is not applicable because the extended systems under investigation exhibit various bonding types and the active site has a larger number of atoms, leading to an poor separation of the trajectories into distinct structures via clustering machine learning algorithms. Therefore, we employed a graph-based analysis within the GaTewAY framework, which accurately distinguishes one structure from another. The unique structures identified from the MD trajectory analysis were subsequently optimized and re-examined using graph theory. Finally, duplicate structures were removed from the graph networks following the procedure described in Section S2. [62].

The structural search procedure outlined in Fig. 2 begins with the exploration of the configurational and reaction space for the zirconocene complex on silica surface using *ab initio* molecular dynamics simulations at the PBE-D3(BJ) level of theory. [57,58,63] It is important to note that standard MD procedures typically provide information only on structures within a single basin of the potential energy surface. [64] To broaden the search, escape techniques must be employed. In this work, we enhance our search with velocity-softening MD simulations. [65] Given that low-energy saddle points often lie at the end of low-curvature modes, [66] this approach allows for rapid escape from the local minimum, even with low-energy trajectories. Within the velocity-softening MD method, the direction of low curvature is determined using an improved dimer method, which relies solely on gradients, thereby eliminating the need for calculating second derivatives. [67] An alternative strategy to facilitate escape from local minima is the application of elevated temperatures, which was also attempted in this work.

Using this enhanced sampling strategy, we started structural search with the organometallic complex positioned atop the SiOH-1 silanol group. The initial graph network, extracted from 10 MD simulations, each comprising 10,000 frames, revealed an ensemble of 295 distinct structures (Fig. S2). Following geometry optimization of each structure, the number of distinct isomers decreased to 33. Subsequent filtering, which excluded species with relative energies exceeding 100 kJ/mol, yielded 25 structures for detailed analysis. Notably, structures were identified that are significantly more stable than the initial guess, with energy reductions of up to 600 kJ/mol.

This reaction network (Fig. 3) can be divided into three parts. The central pathway involves significant surface reconstruction and leads to the formation of a structure that is significantly lower in energy compared to the initial configuration (*vide infra*). The pathways on the left and right involve electrophilic substitution on the Cp rings by silica via a neighboring Si atom in a strained configuration. The structures corresponding to these distinct pathway types are illustrated in

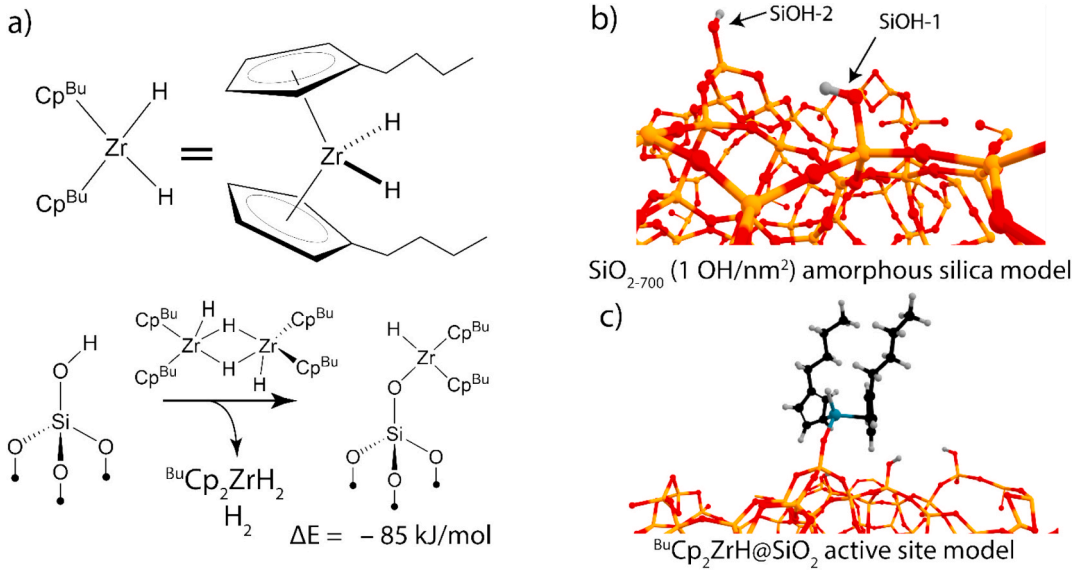

Fig. 1. (a) Formation of the $^{Bu}Cp_2ZrH@SiO_2$ active site. (b) The model representing the amorphous silica surface and the silanol groups considered. (c) The active site model used as a starting point for MD simulations.

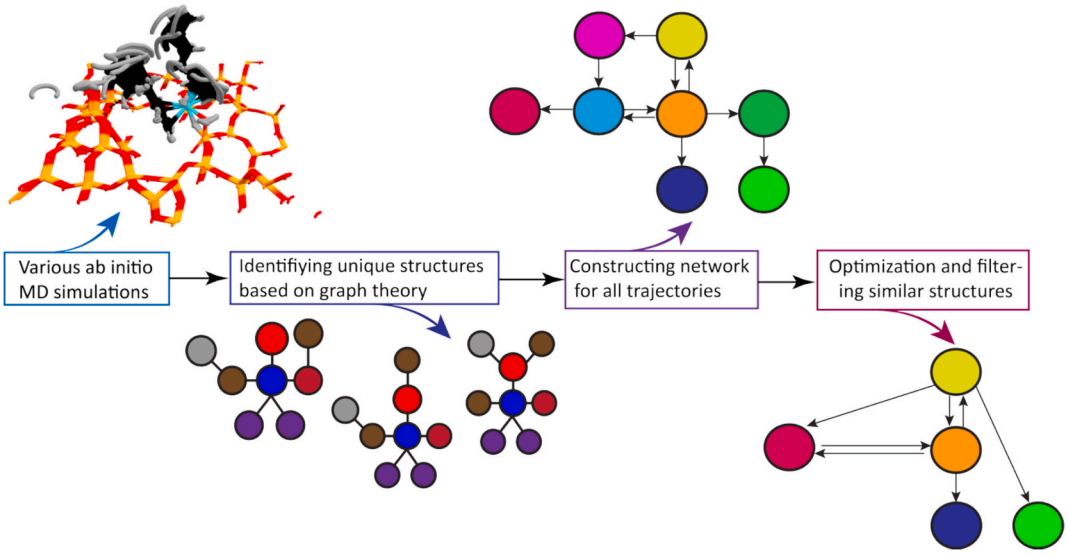

Fig. 2. Schematic representation of the implemented computational workflow.

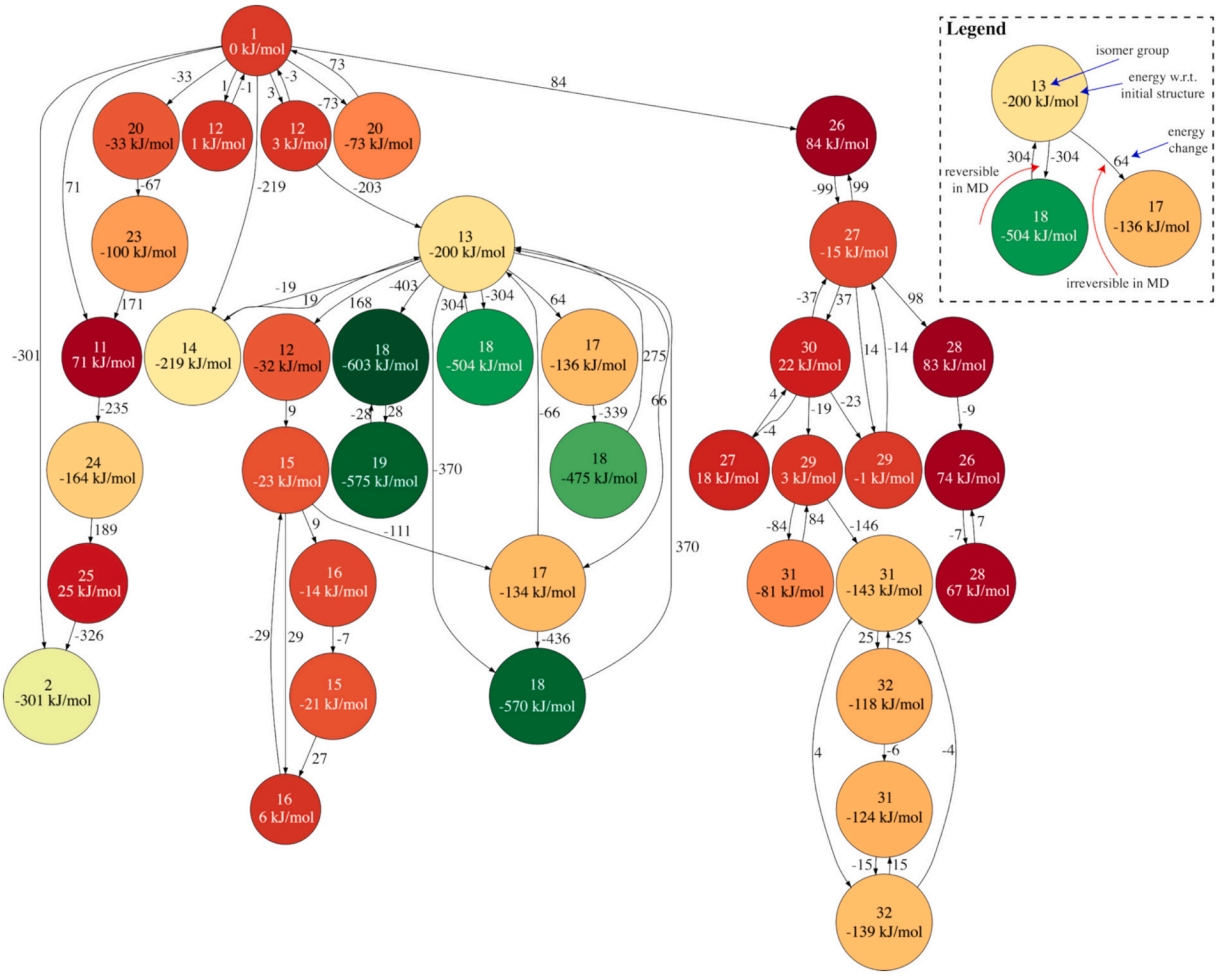

Fig. 3. Active site graph network for the $^{Bu}Cp_2ZrH$@SiOH-1. All relative energies and energy changes are in kJ/mol. All presented energies are for the optimized structures.

Figs. S2–S4. The transformations of other identified paths are summarized in Fig. S3-S5 of the Supplementary Information (SI).

To demonstrate the chemistry behind these graphs, here, we will describe the structural changes along the representative pathway 1 → 12 → 13 → 17 → 18 (numbers correspond to vertices on the graphs, Figs. 3 and 4). The pathway begins with the partial transfer of a hydrogen atom from zirconium to a neighboring silicon atom, resulting in the formation of a Zr…H…Si bridge (transition 1 → 12). This

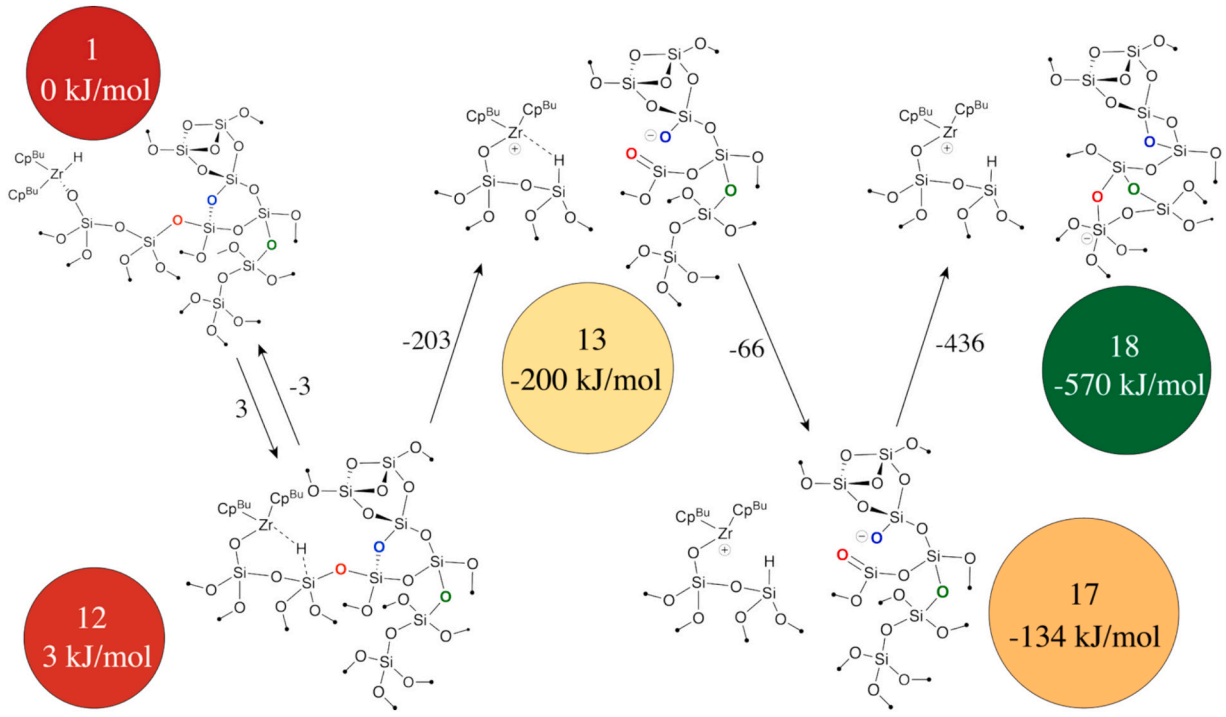

Fig. 4. One of the explored active site transformations of the $^{Bu}Cp_2ZrH$@SiOH-1. The charges shown are assigned based on the chemical intuition to simplify the structure reading.

hydrogen sharing between the coordination spheres of Zr and Si initiates a series of subsequent rearrangements. Next, the opening of a six-membered ring occurs (transition 12 → 13), which leads to the formation of a silanone group (Si=O) and a dangling SiO^- fragment. Hirshfeld spin density analysis confirmed the absence of radical character for these oxygen atoms. Despite the unfavorable nature of the Si=O bond, this step results in a stabilization of 200 kJ/mol. The significant stabilization is attributed to the fact that the silicon atom involved is initially in a highly strained seesaw geometry, making it reactive towards external perturbations; the presence of the zirconocene complex thus may initiate this complex restructuring. The activation barrier for this transformation was calculated to be 13 kJ/mol (see Supporting Information, Section S3), confirming its kinetic accessibility.

Next, the $[^{Bu}Cp_2ZrH]^+$ core rotates around Zr-O bond, thus leaving the hydride outside the coordination sphere of zirconium (13 → 17). In the final transformation (transition 17 → 18), the previously formed defect recombines: the Si=O group interacts with a neighboring SiO_4 tetrahedron yielding a negatively charged, five-coordinated silicon center in a tetragonal bipyramidal geometry. Simultaneously, an oxygen atom (highlighted in green) migrates to an adjacent silicon, resulting in

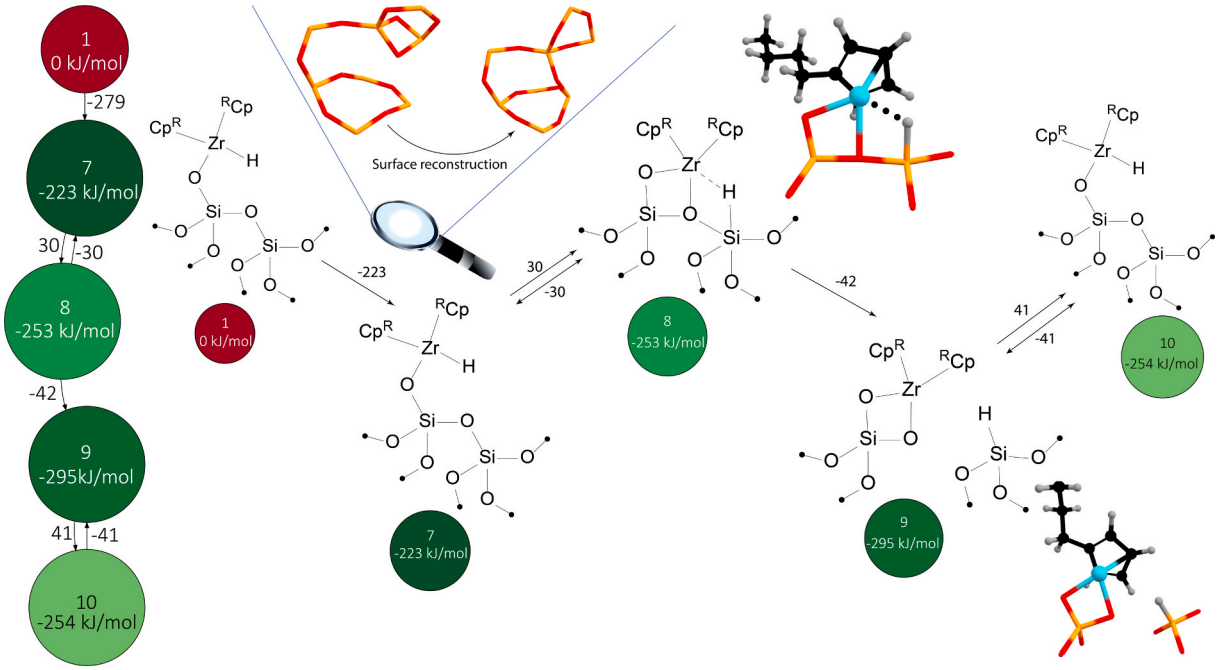

Fig. 5. Discovered active site transformations of the $^{Bu}Cp_2ZrH$@SiOH-2.

the closure of a newly formed three-membered ring. Additionally, the dangling oxygen recombines with another neighboring silicon to form a new siloxane ring. Collectively, these transformations yield a configuration that is significantly stabilized relative to the original structure.

Next, we applied our configurational exploration technique to the $BuCp_2ZrH$@SiOH-2 system, which features a silanol group with less strained local confinement. The graph network after molecular dynamics contains 253 structures, and after applying graph simplification (Section S2) leaves only 12, and of these, only 6 are under the energy cutoff of 100 kJ/mol (Fig. S8). This network is considerably smaller than that obtained for the SiOH-1 system, highlighting how the local confinement of amorphous silica significantly influences the configurational space of the active site. [68] Indeed, because the SiOH-2 group resides in a less strained environment, fewer reaction pathways become accessible.

The chemistry transformation 1 → 10 is summarized in Fig. 5. The initial step in the identified pathway involves surface reorganization to release surface strain. This reorganization transforms the initially strained combination of 2- and 3-membered rings on silica (Si-O-Si-O…) into a configuration featuring a 6-membered ring, which subsequently stabilizes into a combination of two 4-membered rings and one 3-membered ring. This transformation reduces the energy of the system by 245 kJ/mol. Notably, this reorganization also appears to facilitate the formation of an ensemble in which a reversible hydride transfer from Zr to Si can occur.

Thus, by combining reactive molecular dynamics with algorithmic graph theory, we can effectively analyze complex chemical transformations that encompass both modifications of the coordinatively fluxional organometallic core ($[Cp_2ZrH]$) and reorganization of the amorphous surface. The selected surface model is notably strained, which facilitates the initiation of multiple reaction pathways and enhances the diversity of accessible structures.

An interesting question arises regarding the origin of the observed stabilization: while some of the enhanced stability can be attributed to surface relaxation, it is important to quantify the extent of this contribution relative to changes occurring at the organometallic active site. This separation was achieved in the following way:

$$\Delta E_{surf} = E_{surface-after-relaxation} - E_{initial-surface}$$

$$\Delta E_{active} = \Delta E - \Delta E_{surf}$$

where:

ΔE is the energy difference between the considered structure and the initial guess structure.

ΔE_{surf} and ΔE_{active} represents the contribution from the surface and the active site, respectfully.

$E_{surface-after-relaxation}$ is the absolute DFT energy of the surface of the considered structure after relaxation, with the $[^{Bu}Cp_2ZrH]^+$ moiety replaced by a proton followed by optimization.

$E_{initial-surface}$ is the absolute DFT energy of the initial surface.

Fig. 6 represents a visual representation of ΔE (red line) and ΔE_{active} (blue line). When the red line lies above the blue line ($\Delta E_{active} < \Delta E$), it indicates that surface relaxation contributes to the overall stabilization. This behavior is observed for most of the structures in our study. In many cases, for structures that are lower in energy than the initial guess, the value of ΔE_{active} suggests that their enhanced stability is primarily due to surface reconstruction. However, in some instances, such as for structures 18 and 19, ΔE_{active} is around −200 kJ/mol, implying that both surface strain and active site transformations contribute to the overall stabilization.

4. Conclusions

In this study, we examined the configurational space of organometallic catalysts supported on amorphous materials, using 1,1′-bis(n-butyl-cyclopentadienyl)zirconium hydride on amorphous silica as a case system. To achieve this, we designed a computational workflow for exploring active site configurations. The exploration algorithm consists of several steps. First, (reactive) MD simulations are run to ensure that the trajectories escape the basin of the initial local minima, thereby enabling a broader sampling of the potential energy surface. Next, a graph theory–based MD post-processing tool GaTewAY is used to identify unique isomers, constructing an ensemble that reveals how different structures interconvert. Finally, the structures extracted from the MD trajectories are optimized, and a subsequent graph theory analysis is performed to refine the results.

By applying this combined approach to the $^{Bu}Cp_2ZrH_2$@SiO_2 system, we have shown that differences in the local environment of the silica model, such as the degree of strain around different silanol sites, can significantly influence the configurational space and reaction pathways available to the active site. For instance, systems anchored on silanol groups with strained confinement yield a diverse ensemble of structures and transformation pathways, with surface reconstruction contributing to the stabilization by up to several hundred kJ/mol. In contrast, catalysts supported on SiOH-2, which is characterized by less strained confinement, exhibit a more restricted set of accessible configurations.

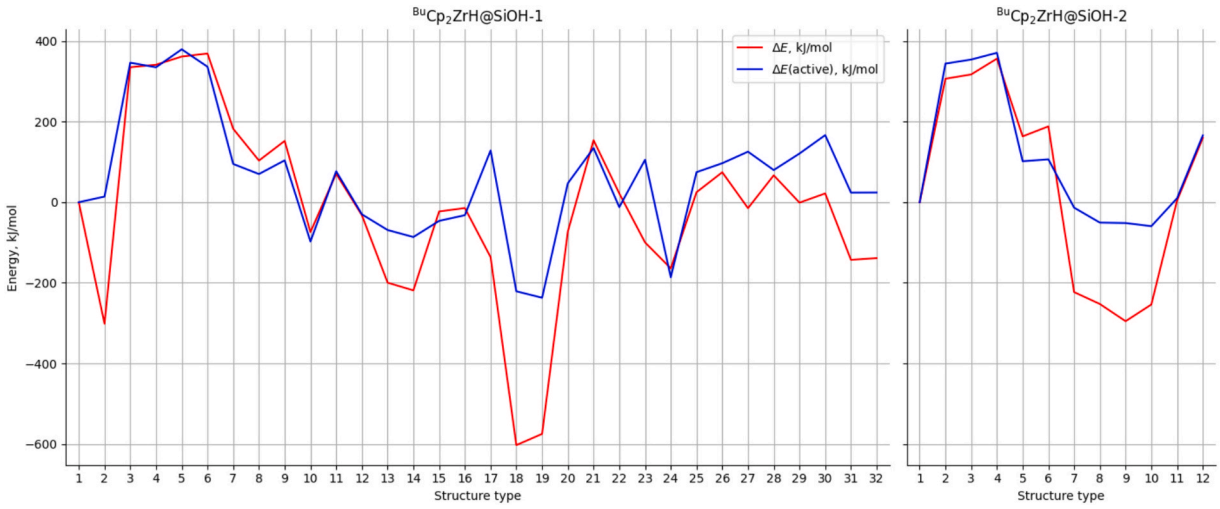

Fig. 6. Line plot depicting the relative energies (ΔE, kJ/mol) and active site contribution energies (ΔE_{active}, kJ/mol) for structures discovered with our algorithm starting from $^{Bu}Cp_2ZrH$@SiOH-1 (left) and $^{Bu}Cp_2ZrH$@SiOH-2 (right).

Most importantly, our study demonstrates that integrating (reactive) molecular dynamics with graph theory-based analysis offers an intuitive and chemically meaningful approach to unravel the complex, fluxional behavior of surface organometallic catalysts on amorphous supports.

5. Associated Content

Supporting Information

Additional data regarding the MD postprocessing (pdf). The Cartesian coordinates of the optimized structures extracted from the molecular dynamics (.zip). The complete dataset (trajectories, structures in the.xyz format, numerical data, output files) will be available at the moment of the publication at 4TU.nl data repository under DOI https://doi.org/10.4121/dabeda0b-fd48-4ebd-ad0f-3c9fa769c731. The python code for graphs postprocessing and visualizing is available at GitHub: https://github.com/aakolganov/GatGraphProc.

Funding sources

The use of the supercomputer resources (Snellius) was sponsored by NWO domain science.

CRediT authorship contribution statement

Alexander A. Kolganov: Writing – review & editing, Writing – original draft, Visualization, Methodology, Formal analysis, Data curation, Conceptualization. **Sana Bouguerroua:** Writing – review & editing, Software, Methodology, Formal analysis. **Marie-Pierre Gaigeot:** Writing – review & editing, Supervision. **Matthew P. Conley:** Writing – review & editing, Supervision. **Evgeny A. Pidko:** Writing – review & editing, Supervision, Funding acquisition, Conceptualization.

Declaration of competing interest

The authors declare that they have no known competing financial interests or personal relationships that could have appeared to influence the work reported in this paper.

Appendix A. Supplementary data

Supplementary data to this article can be found online at https://doi.org/10.1016/j.jcat.2025.116521.

Data availability

The complete dataset is available at 4TU data repository under DOI: https://doi.org/10.4121/dabeda0b-fd48-4ebd-ad0f-3c9fa769c731.

References

[1] C. Vogt, B.M. Weckhuysen, The concept of active site in heterogeneous catalysis, Nat. Rev. Chem. 6 (2) (2022) 89–111, https://doi.org/10.1038/s41570-021-00340-y.
[2] F. Studt, Grand challenges in computational catalysis, Front. Catal. 1 (2021) 658965, https://doi.org/10.3389/fctls.2021.658965.
[3] S.R. Gathmann, M.A. Ardagh, P.J. Dauenhauer, Catalytic resonance theory: negative dynamic surfaces for programmable catalysts, Chem Catal. 2 (1) (2022) 140–163, https://doi.org/10.1016/j.checat.2021.12.006.
[4] M.H. Ning, S.N. Wang, J. Wan, Z.C. Xi, Q. Chen, Y.M. Sun, H. Li, T.Y. Ma, H.Y. Jin, Dynamic active sites in electrocatalysis, Angew. Chem. Int. Ed. 63 (50) (2024) e202415794, https://doi.org/10.1002/anie.202415794.
[5] H. Zhang, L. Chen, F. Dong, Z.W. Lu, E.M. Lv, X.L. Dong, H.X. Li, Z.Y. Yuan, X. W. Peng, S.H. Yang, et al., Dynamic transformation of active sites in energy and environmental catalysis, Energ. Environ. Sci. 17 (18) (2024) 6435–6481, https://doi.org/10.1039/d4ee02365j.
[6] M.A. Ardagh, M. Shetty, A. Kuznetsov, Q. Zhang, P. Christopher, D.G. Vlachos, O. A. Abdelrahman, P.J. Dauenhauer, Catalytic resonance theory: parallel reaction pathway control, Chem. Sci. 11 (13) (2020) 3501–3510, https://doi.org/10.1039/c9sc06140a.
[7] D.P. Zhang, Y.X. Li, P.F. Wang, J.Y. Qu, Y. Li, S.H. Zhan, Dynamic active-site induced by host-guest interactions boost the Fenton-like reaction for organic wastewater treatment, Nat. Commun. 14 (1) (2023) 3538, https://doi.org/10.1038/s41467-023-39228-4.
[8] Z. Zhang, B. Zandkarimi, A.N. Alexandrova, Ensembles of Metastable States govern Heterogeneous Catalysis on Dynamic Interfaces, Acc. Chem. Res. 53 (2) (2020) 447–458, https://doi.org/10.1021/acs.accounts.9b00531.
[9] R.H. Lavroff, H.W.T. Morgan, Z. Zhang, P. Poths, A.N. Alexandrova, Ensemble representation of catalytic interfaces: soloists, orchestras, and everything in-between, Chem. Sci. 13 (27) (2022) 8003–8016, https://doi.org/10.1039/D2SC01367C.
[10] S. Kar, D. Milstein, Sustainable catalysis with fluxional acridine-based PNP pincer complexes, Chem. Commun. 58 (23) (2022) 3731–3746, https://doi.org/10.1039/D2CC00247G.
[11] A.K. Jain, M.R. Gau, P.J. Carroll, K.I. Goldberg, Comparing square-planar RhI and IrI: metal–ligand proton tautomerism, fluxionality, and reactivity, Organometallics 41 (22) (2022) 3341–3348, https://doi.org/10.1021/acs.organomet.2c00302.
[12] Y.L. Li, H.L. Wang, Z.H. Zhu, Y.F. Wang, F.P. Liang, H.H. Zou, Aggregation induced emission dynamic chiral europium(III) complexes with excellent circularly polarized luminescence and smart sensors, Nat. Commun. 15 (1) (2024), https://doi.org/10.1038/s41467-024-47246-z.
[13] F.A. Cotton, D.L. Hunter, P. Lahuerta, Fluxional organometal carbonyl molecule with several scrambling processes - C-13 nuclear magnetic-resonance study of (Eta-6-Cyclooctatriene)(Hexacarbonyl)Diiron(Fe-Fe), J. Am. Chem. Soc. 97 (5) (1975) 1046–1050, https://doi.org/10.1021/ja00838a016.
[14] D. Laurencin, E.G. Fidalgo, R. Villanneau, F. Villain, P. Herson, J. Pacifico, H. Stoeckli-Evans, M. Bénard, M.M. Rohmer, G. Süss-Fink, et al., Framework fluxionality of organometallic oxides:: Synthesis, crystal structure, EXAFS, and DFT studies on [{Ru(η-arene)}MoO] complexe, Chem. Eur. J. 10 (1) (2004) 208–217, https://doi.org/10.1002/chem.200305396.
[15] A. Macchioni, Ion pairing in transition-metal organometallic chemistry, Chem. Rev. 105 (6) (2005) 2039–2074, https://doi.org/10.1021/cr0300439.
[16] P. Vidossich, A. Lledós, G. Ujaque, First-Principles Molecular Dynamics Studies of Organometallic Complexes and Homogeneous Catalytic Processes, Acc. Chem. Res. 49 (6) (2016) 1271–1278, https://doi.org/10.1021/acs.accounts.6b00054.
[17] Orrell, K. G.; Šik, V. Dynamic NMR Spectroscopy in Inorganic and Organometallic Chemistry. In *Annual Reports on NMR Spectroscopy*, Webb, G. A. Ed.; Vol. 27; Academic Press, 1993; pp 103-171.
[18] B.R. Goldsmith, B. Peters, J.K. Johnson, B.C. Gates, S.L. Scott, Beyond ordered materials: understanding catalytic sites on amorphous solids, ACS Catal. 7 (11) (2017) 7543–7557, https://doi.org/10.1021/acscatal.7b01767.
[19] C. Copéret, A. Comas-Vives, M.P. Conley, D.P. Estes, A. Fedorov, V. Mougel, H. Nagae, F. Núñez-Zarur, P.A. Zhizhko, Surface organometallic and coordination chemistry toward single-site heterogeneous catalysts: strategies, methods, structures, and activities, Chem. Rev. 116 (2) (2016) 323–421, https://doi.org/10.1021/acs.chemrev.5b00373.
[20] X. Rozanska, F. Delbecq, P. Sautet, Reconstruction and stability of β-cristobalite 001, 101, and 111 surfaces during dehydroxylation, Phys. Chem. Chem. Phys. 12 (45) (2010) 14930–14940, https://doi.org/10.1039/C0CP00287A.
[21] G. Li, P. Vassilev, M. Sanchez-Sanchez, J.A. Lercher, E.J.M. Hensen, E.A. Pidko, Stability and reactivity of copper oxo-clusters in ZSM-5 zeolite for selective methane oxidation to methanol, J. Catal. 338 (2016) 305–312, https://doi.org/10.1016/j.jcat.2016.03.014.
[22] A.A. Kolganov, A.A. Gabrienko, I.Y. Chernyshov, A.G. Stepanov, E.A. Pidko, Property–activity relations of multifunctional reactive ensembles in cation-exchanged zeolites: a case study of methane activation on Zn2+-modified zeolite BEA, Phys. Chem. Chem. Phys. 24 (11) (2022) 6492–6504, https://doi.org/10.1039/D1CP05854A.
[23] J.T. Margraf, H. Jung, C. Scheurer, K. Reuter, Exploring catalytic reaction networks with machine learning, Nat. Catal. 6 (2) (2023) 112–121, https://doi.org/10.1038/s41929-022-00896-y.
[24] M. Steiner, M. Reiher, Autonomous Reaction Network Exploration in Homogeneous and Heterogeneous Catalysis, Top. Catal. 65 (1) (2022) 6–39, https://doi.org/10.1007/s11244-021-01543-9.
[25] B. Hartke, Global optimization, WIREs Comput. Mol. Sci. 1 (6) (2011) 879–887, https://doi.org/10.1002/wcms.70.
[26] S. Heiles, R.L. Johnston, Global optimization of clusters using electronic structure methods, Int. J. Quant. Chem. 113 (18) (2013) 2091–2109, https://doi.org/10.1002/qua.24462.
[27] D. Wales, Energy Landscapes: Applications to Clusters, Biomolecules and Glasses, Cambridge University Press, 2004, https://doi.org/10.1017/CBO9780511721724.
[28] H. Zhai, M.-A. Ha, A.N. Alexandrova, AFFCK: adaptive force-field-assisted ab initio coalescence kick method for global minimum search, J. Chem. Theory Comput. 11 (5) (2015) 2385–2393, https://doi.org/10.1021/acs.jctc.5b00065.
[29] A.N. Alexandrova, H·(H2O)n clusters: microsolvation of the hydrogen atom via molecular ab initio gradient embedded genetic algorithm (GEGA), Chem. Eur. J. 114 (48) (2010) 12591–12599, https://doi.org/10.1021/jp1092543.
[30] A.N. Alexandrova, A.I. Boldyrev, Search for the Lin0/+1/-1 (n = 5−7) Lowest-Energy Structures using the ab Initio Gradient embedded Genetic Algorithm (GEGA). Elucidation of the Chemical Bonding in the Lithium Clusters, J. Chem. Theory Comput. 1 (4) (2005) 566–580, https://doi.org/10.1021/ct050093g.
[31] Y. Wang, J. Lv, L. Zhu, Y. Ma, CALYPSO: a method for crystal structure prediction, Comput. Phys. Commun. 183 (10) (2012) 2063–2070, https://doi.org/10.1016/j.cpc.2012.05.008.
[32] G.G. Rondina, J.L.F. Da Silva, Revised Basin-Hopping Monte Carlo algorithm for structure optimization of clusters and nanoparticles, J. Chem. Inf. Model. 53 (9) (2013) 2282–2298, https://doi.org/10.1021/ci400224z.

[33] D.J. Wales, J.P.K. Doye, Global optimization by basin-hopping and the lowest energy structures of Lennard-Jones clusters containing up to 110 atoms, Chem. Eur. J. 101 (28) (1997) 5111–5116, https://doi.org/10.1021/jp970984n.
[34] Z. Zhang, W. Gee, R.H. Lavroff, A.N. Alexandrova, GOCIA: grand canonical global optimizer for clusters, interfaces, and adsorbates, Phys. Chem. Chem. Phys. 27 (2) (2025) 696–706, https://doi.org/10.1039/D4CP03801K.
[35] S. Maeda, Y. Harabuchi, M. Takagi, T. Taketsugu, K. Morokuma, Artificial Force Induced Reaction (AFIR) Method for Exploring Quantum Chemical potential Energy Surfaces, Chem. Rec. 16 (5) (2016) 2232–2248, https://doi.org/10.1002/tcr.201600043.
[36] S. Maeda, K. Ohno, K. Morokuma, Systematic exploration of the mechanism of chemical reactions: the global reaction route mapping (GRRM) strategy using the ADDF and AFIR methods, Phys. Chem. Chem. Phys. 15 (11) (2013) 3683–3701, https://doi.org/10.1039/C3CP44063J.
[37] S. Maeda, Y. Harabuchi, M. Takagi, K. Saita, K. Suzuki, T. Ichino, Y. Sumiya, K. Sugiyama, Y. Ono, Implementation and performance of the artificial force induced reaction method in the GRRM17 program, J. Comput. Chem. 39 (4) (2018) 233–251, https://doi.org/10.1002/jcc.25106 (acccessed 2024/08/29).
[38] G.M. Piccini, M.S. Lee, S.F. Yuk, D.F. Zhang, G. Collinge, L. Kollias, M.T. Nguyen, V.A. Glezakou, R. Rousseau, molecular dynamics with enhanced sampling in heterogeneous catalysis, Cat. Sci. Technol. 12 (1) (2022) 12–37, https://doi.org/10.1039/d1cy01329g.
[39] E. Martínez-Núñez, An automated transition state search using classical trajectories initialized at multiple minima, Phys. Chem. Chem. Phys. 17 (22) (2015) 14912–14921, https://doi.org/10.1039/c5cp02175h.
[40] B. Ensing, M. De Vivo, Z.W. Liu, P. Moore, M.L. Klein, Metadynamics as a tool for exploring free energy landscapes of chemical reactions, Acc. Chem. Res. 39 (2) (2006) 73–81, https://doi.org/10.1021/ar040198i.
[41] R.J. Shannon, E. Martínez-Núñez, D.V. Shalashilin, D.R. Glowacki, ChemDyME: Kinetically Steered, Automated Mechanism Generation through combined Molecular Dynamics and Master Equation Calculations, J. Chem. Theory Comput. 17 (8) (2021) 4901–4912, https://doi.org/10.1021/acs.jctc.1c00335.
[42] J. Vandermause, Y. Xie, J.S. Lim, C.J. Owen, B. Kozinsky, Active learning of reactive Bayesian force fields applied to heterogeneous catalysis dynamics of H/Pt, Nat. Commun. 13 (1) (2022) 5183, https://doi.org/10.1038/s41467-022-32294-0.
[43] S. Bougueroua, Y. Aboulfath, D. Barth, M.-P. Gaigeot, Algorithmic graph theory for post-processing molecular dynamics trajectories, Mol. Phys. 121 (7–8) (2023) e2162456, https://doi.org/10.1080/00268976.2022.2162456.
[44] S. Bougueroua, A.A. Kolganov, C. Helain, C. Zens, D. Barth, E.A. Pidko, M.-P. Gaigeot, Exploiting graph theory in MD simulations for extracting chemical and physical properties of materials, Phys. Chem. Chem. Phys. 27 (3) (2025) 1298–1309, https://doi.org/10.1039/D4CP02764G.
[45] S. Bougueroua, R. Spezia, S. Pezzotti, S. Vial, F. Quessette, D. Barth, M.P. Gaigeot, Graph theory for automatic structural recognition in molecular dynamics simulations, J. Chem. Phys. 149 (18) (2018) 184102, https://doi.org/10.1063/1.5045818.
[46] S. Bougueroua, M. Bricage, Y. Aboulfath, D. Barth, M.-P. Gaigeot, Algorithmic graph theory, reinforcement learning and game theory in MD simulations: from 3D structures to topological 2D-molecular graphs (2D-MolGraphs) and vice versa, Molecules 28 (7) (2023) 2892, https://doi.org/10.3390/molecules28072892.
[47] A. Hashemi, S. Bougueroua, M.-P. Gaigeot, E.A. Pidko, ReNeGate: a Reaction Network Graph-Theoretical Tool for Automated Mechanistic Studies in Computational Homogeneous Catalysis, J. Chem. Theory Comput. 18 (12) (2022) 7470–7482, https://doi.org/10.1021/acs.jctc.2c00404.
[48] Y. Aboulfath, S. Bougueroua, A. Cimas, D. Barth, M.-P. Gaigeot, Time-Resolved Graphs of Polymorphic Cycles for H-Bonded Network Identification in Flexible Biomolecules, J. Chem. Theory Comput. 20 (3) (2024) 1019–1035, https://doi.org/10.1021/acs.jctc.3c01031.
[49] A.T. Balaban, Applications of graph theory in chemistry, J. Chem. Inf. Comput. Sci. 25 (3) (1985) 334–343, https://doi.org/10.1021/ci00047a033.
[50] D.B. Culver, R.W. Dorn, A. Venkatesh, J. Meeprasert, A.J. Rossini, E.A. Pidko, A. S. Lipton, G.R. Lief, M.P. Conley, Active Sites in a Heterogeneous Organometallic Catalyst for the Polymerization of Ethylene, ACS Cent. Sci. 7 (7) (2021) 1225–1231, https://doi.org/10.1021/acscentsci.1c00466.
[51] F.D. Cannavacciuolo, R. Yadav, A. Esper, A. Vittoria, G. Antinucci, F. Zaccaria, R. Cipullo, P.H.M. Budzelaar, V. Busico, G.P. Goryunov, et al., A High-Throughput Approach to Repurposing Olefin Polymerization Catalysts for Polymer Upcycling, Angew. Chem. Int. Ed. 61 (23) (2022) e202202258, https://doi.org/10.1002/anie.202202258.
[52] J. Sun, J. Dong, L. Gao, Y.-Q. Zhao, H. Moon, S.L. Scott, Catalytic Upcycling of Polyolefins, Chem. Rev. 124 (16) (2024) 9457–9579, https://doi.org/10.1021/acs.chemrev.3c00943.
[53] K.K. Samudrala, M.P. Conley, A Supported Ziegler-Type Organohafnium Site Metabolizes Polypropylene, J. Am. Chem. Soc. 145 (45) (2023) 24447–24451, https://doi.org/10.1021/jacs.3c05940.
[54] A. Comas-Vives, Amorphous SiO_2 surface models: energetics of the dehydroxylation process, strain, ab initio atomistic thermodynamics and IR spectroscopic signatures, Phys. Chem. Chem. Phys. 18 (10) (2016) 7475–7482, https://doi.org/10.1039/C6CP00602G.
[55] T.D. Kühne, M. Iannuzzi, M. Del Ben, V.V. Rybkin, P. Seewald, F. Stein, T. Laino, R. Z. Khaliullin, O. Schütt, F. Schiffmann, et al., CP2K: an electronic structure and molecular dynamics software package - Quickstep: Efficient and accurate electronic structure calculations, J. Chem. Phys. 152 (19) (2020) 194103, https://doi.org/10.1063/5.0007045.
[56] G. Lippert, J. Hutter, M. Parrinello, A hybrid Gaussian and plane wave density functional scheme, Mol. Phys. 92 (3) (1997) 477–487, https://doi.org/10.1080/002689797094821l9.
[57] J.P. Perdew, K. Burke, M. Ernzerhof, Generalized Gradient Approximation made simple, Phys. Rev. Lett. 77 (18) (1996) 3865–3868, https://doi.org/10.1103/PhysRevLett.77.3865.
[58] S. Grimme, S. Ehrlich, L. Goerigk, Effect of the damping function in dispersion corrected density functional theory, J. Comput. Chem. 32 (7) (2011) 1456–1465, https://doi.org/10.1002/jcc.21759.
[59] J. VandeVondele, J. Hutter, Gaussian basis sets for accurate calculations on molecular systems in gas and condensed phases, J. Chem. Phys. 127 (11) (2007) 114105, https://doi.org/10.1063/1.2770708.
[60] J. Hutter, M. Iannuzzi, F. Schiffmann, J. VandeVondele, cp2k: atomistic simulations of condensed matter systems, WIREs Comput. Mol. Sci. 4 (1) (2014) 15–25, https://doi.org/10.1002/wcms.1159.
[61] E.V. Khramenkova, M.G. Medvedev, G. Li, E.A. Pidko, Unraveling the Nature of Extraframework Catalytic Ensembles in Zeolites: Flexibility and Dynamics of the Copper-Oxo Trimers in Mordenite, J. Phys. Chem. Lett. 12 (44) (2021) 10906–10913, https://doi.org/10.1021/acs.jpclett.1c03288.
[62] A. Hashemi, S. Bougueroua, M.-P. Gaigeot, E.A. Pidko, HiREX: High-Throughput Reactivity Exploration for Extended Databases of Transition-Metal Catalysts, J. Chem. Inf. Model. 63 (19) (2023) 6081–6094, https://doi.org/10.1021/acs.jcim.3c00660.
[63] S. Grimme, J. Antony, S. Ehrlich, H. Krieg, A consistent and accurate ab initio parametrization of density functional dispersion correction (DFT-D) for the 94 elements H-Pu, J. Chem. Phys. 132 (15) (2010) 154104, https://doi.org/10.1063/1.3382344.
[64] A. Laio, M. Parrinello, Escaping free-energy minima, Proc. Natl. Acad. Sci. 99 (20) (2002) 12562–12566, https://doi.org/10.1073/pnas.202427399.
[65] S.E. Schönborn, S. Goedecker, S. Roy, A.R. Oganov, The performance of minima hopping and evolutionary algorithms for cluster structure prediction, J. Chem. Phys. 130 (14) (2009) 144108, https://doi.org/10.1063/1.3097197.
[66] S. Roy, S. Goedecker, V. Hellmann, Bell-Evans-Polanyi principle for molecular dynamics trajectories and its implications for global optimization, Phys. Rev. E 77 (5) (2008) 056707, https://doi.org/10.1103/PhysRevE.77.056707.
[67] G. Henkelman, H. Jónsson, A dimer method for finding saddle points on high dimensional potential surfaces using only first derivatives, J. Chem. Phys. 111 (15) (1999) 7010–7022, https://doi.org/10.1063/1.480097.
[68] C.S. Praveen, A.P. Borosy, C. Copéret, A. Comas-Vives, Strain in Silica-Supported Ga(III) Sites: neither too much nor too Little for Propane Dehydrogenation Catalytic activity, Inorg. Chem. 60 (10) (2021) 6865–6874, https://doi.org/10.1021/acs.inorgchem.0c03135.